Polymorphic Gompertzian model of cancer validated with *in vitro* and *in vivo* data

Arina Soboleva[a,b], Artem Kaznatcheev[c], Rachel Cavill[b], Katharina Schneider[b], Kateřina Staňková[a]

[a] *Institute for Health Systems Science, Faculty of Technology, Policy and Management, Delft University of Technology, Delft, The Netherlands*
[b] *Department of Advanced Computing Sciences, Faculty of Science and Engineering, Maastricht University, Maastricht, The Netherlands*
[c] *Department of Mathematics and Department of Information and Computing Sciences, Utrecht University, Utrecht, The Netherlands*

Abstract

Mathematical modeling plays an important role in our understanding of therapy resistance mechanisms in cancer. The polymorphic Gompertzian model, analyzed theoretically by Viossat and Noble, describes a heterogeneous cancer population consisting of therapy sensitive and resistant cells. This theoretically promising model has not previously been validated with real-world data. In this study, we provide this validation. We demonstrate that the polymorphic Gompertzian model successfully captures trends in both *in vitro* and *in vivo* data on non-small cell lung cancer (NSCLC) dynamics under treatment. For the *in vivo* data of tumor dynamics in patients undergoing treatment, we compare the polymorphic Gompertzian model to the classical oncologic models, which were previously identified as the models fitting this data the best. We showed that the polymorphic Gompertzian model can successfully capture the U-shape trend in tumor size during cancer relapse, which can not be fitted with the classical oncologic models. In general, the polymorphic Gompertzian model corresponds well to both *in vitro* and *in vivo* real-world data, suggesting it as a candidate for improving the efficacy of cancer therapy, for example through evolutionary/adaptive therapies.

Keywords: Mathematical Oncology, Model validation, Polymorphic Gompertzian model, Non-Small Cell Lung Cancer, Anti-cancer therapy

---

1. Introduction

For patients with advanced cancer, an aggressive treatment, aiming at complete cancer eradication, is often ineffective [1, 2]. Instead of pursuing tumor elimination through maximum tolerable dose, novel therapies – termed evolutionary therapies – aim at creating more complex time- and tumor-dependent treatment schedules that anticipate and steer cancer eco-evolutionary dynamics in response to the treatment [2–15]. Mathematical models of cancer's response to therapy may help us to guide such therapies and, perhaps even more importantly, are needed to understand conditions under which the evolutionary therapies outperform standard of care [5, 16–25].

Recently, Viossat and Noble [26] analyzed a group of density-dependent polymorphic models assuming two types of cancer cells, therapy-resistant and therapy-sensitive ones, and demonstrated that Zhang's adaptive therapy protocol [5, 24] outperforms standard treatment in all these models in terms of time to progression. Their numerical simulations were performed on one of these models, a two-population Gompertzian model. The model assumes equal growth rates for the sensitive and resistant populations, density-dependent selection, and no cost of resistance, i.e. no assumption that resistant cells are less fit than the sensitive ones when therapy is not applied [14, 27–29]. The model assumes no direct competition between different cell types through competition coefficients, but a shared carrying capacity instead. The absence of the cost of resistance makes the model applicable to a wider range of cancer types, as it was suggested that in some cancers, resistance does not need to have a cost [5, 27, 30, 31].

Viossat and Noble [26] show that in the polymorphic Gompertzian model, adaptive treatment protocols increase time to progression compared to the continuous application of maximum tolerable dose. However, before bringing these models to clinical practice, their ability to fit the real-world data should be evaluated [32, 33]. In this study, we aim to test the polymorphic Gompertzian model's agreement with *in vitro* data from Kaznatcheev et al. [30] and *in vivo* data from previous clinical studies [34–38] of non-small cell lung cancer (NSCLC) dynamics under therapy.

2. Methods

The polymorphic Gompertzian model of cancer analyzed by Viossat and Noble [26] assumes two types of cancer cell populations - sensitive and re-

sistant to treatment - with sizes $S(t)$ and $R(t)$ at time t, respectively. The total size of cancer population at time t is $N(t) = S(t) + R(t)$. The dynamics of the two populations are described by the ordinary differential equations:

$$\dot{S}(t) = \rho \ln\left(\frac{K}{N(t)}\right)(1 - \lambda C(t))S(t) \tag{1}$$

$$\dot{R}(t) = \rho \ln\left(\frac{K}{N(t)}\right)R(t), \tag{2}$$

where $C(t)$ is treatment dosage at time t, K is carrying capacity of the tumor (that defines maximum possible size to which the cancer population can grow), ρ is growth rate of cancer cells, and λ is treatment sensitivity.

Note that competition between sensitive and resistant cells is not explicitly present in the model, besides competing for the space limited by the carrying capacity. The model also assumes the same growth rate ρ for both populations. Thus, in this model, therapy resistance does not have a cost.

2.1. Fitting the model to in vitro data

We first validated the polymorphic Gompertzian model on *in vitro* data from the study by Kaznatcheev et al. [30]. In their study, two populations of NSCLC cells - sensitive and resistant to treatment - were seeded at different initial proportions with and without addition of cancer-associated fibroblasts (CAF) and the immunotherapy drug Alectinib. In total, the data contains 192 wells: eight different intended initial proportions of sensitive cells (0, 0.1, 0.2, 0.4, 0.6, 0.8, 0.9, 1) in four conditions (Drug-, CAF-; Drug-, CAF+; Drug+, CAF-; Drug+, CAF+) and six replicates for each combination. For all wells, sizes of sensitive and resistant populations over time are presented.

We fitted the population dynamics of sensitive and resistant cells for each of the 192 wells to the polymorphic Gompertzian model using the Python GEKKO package [39] with mean squared error as the objective function:

$$MSE_S = \frac{1}{n}\sum_{i=1}^{n}(S_{pred}(t_i) - S_{mes}(t_i))^2 \tag{3}$$

$$MSE_R = \frac{1}{n}\sum_{i=1}^{n}(R_{pred}(t_i) - R_{mes}(t_i))^2, \tag{4}$$

where $S_{mes}(t_i)$ and $R_{mes}(t_i)$ are measured sizes of sensitive and resistant populations at i-th time point, $S_{pred}(t_i)$ and $R_{pred}(t_i)$ are model-predicted

sensitive and resistant population sizes at i-th time point, and n is the number of time points.

In the fitting procedure, we exploited the explicit treatment modelling through variable $C(t_i)$, the treatment dosage at discretized time t_i. In wells where the drug was not applied, we set $C(t_i) = 0$ for all t_i. The dynamics in wells with drug were modeled as the treatment variable $C(t_i)$ set to 0 in time points $t_i < 20$ hours and to 1 at time points $t_i \geq 20$ hours. This way, we reflected the conditions of the experiment, where Alectinib was added to the wells 20 hours after seeding [30]. As CAF have a variety of functions and action mechanisms [40], which are challenging for direct modeling, we evaluated the effect of CAF implicitly through a comparison of the fitted model's parameters values (K, ρ, λ) in wells with and without CAF. In the wells with seeding proportions 0 and 1 (fully resistant and sensitive wells), we set the measurements of the minor population to zero before fitting the model, as they present solely fluorescent noise. The obtained parameter values and their dependence on the initial proportions of sensitive cells and experimental conditions were analyzed.

2.2. Fitting the model to in vivo data

We used data from clinical trials of NSCLC patients treated with either immunotherapy drug Atezolizumab or chemotherapy drug Docetaxel [34–38]. The data contains measurements of the longest diameters of lesions over time, assessed through CT scans. We estimated the volume of the target tumor, following the common assumption that the tumor is a sphere with a diameter equal to the longest measured lesion diameter [41].

Focusing on the tumors with six or more measurements over time, we split the resultant 587 patient cases into five categories based on the trend in the measured data: "Growth", "Decline", "Delayed response", "U-shape" or "Fluctuate" (For details, see Appendix B). We fitted the polymorphic Gompertzian model to the tumor volumes of each of the 587 patients using the Python package GEKKO [39] with MSE between measured data and the sum of model-predicted sensitive and resistant population sizes as the objective function:

$$MSE = \frac{1}{n} \sum_{i=1}^{n} \left((R_{pred}(t_i) + S_{pred}(t_i)) - x_{mes}(t_i) \right)^2 , \tag{5}$$

where $x_{mes}(t_i)$ is measured tumor volume at i-th time point, $R_{pred}(t_i)$ and

$S_{pred}(t_i)$ are model-predicted resistant and sensitive population volumes at i-th time point, and n is number of time points.

As the *in vivo* data contains only total population sizes, initial proportions of sensitive cells were established (See Appendix A). We modeled the treatment as a constant function $C(t_i) = 1$, as in the clinical studies patients received chemotherapy or immunotherapy regularly and in the same dosage [35–38]. After obtaining the model's fits we assessed the parameters of the model and the accuracy of the fit in different trend categories (See Appendix D). We also fitted two best performing classical models of Laleh's et al.'s study [34] - General Gompertz and General von Bertalanffy models - to the *in vivo* data and compared accuracy of the three models within the trend categories (See Appendix C).

3. Results

3.1. In vitro data

3.1.1. The fit of the polymorphic Gompertzian model to data dynamics

We fitted the polymorphic Gompertzian model to *in vitro* dynamics of sensitive and resistant cancer populations. The model's fit to the measured data in four experimental conditions (Drug-, CAF-; Drug-, CAF+; Drug+, CAF-; Drug+, CAF+) and with seeding proportions of sensitive cells is presented in Fig. 1. Columns represent the experimental conditions of wells. Each row contains wells from one of the proportion groups (0.2, 0.4, 0.6, 0.8) corresponding to the seeding proportions of sensitive cells. The actual proportions in wells differ from the intended ones due to experimental variations.

The trend dynamics were captured well for all experimental and initial conditions. In particular, the model reflected the convex form of the population growth with a slowing of the growth rate closer to a larger size (rows $3-4$ of Fig. 1). We modeled the therapy start at $t_i = 20h$ following the experimental setting and, thus, were able to capture the change of the trend in the sensitive population (columns $3-4$ of Fig. 1). The population initially was growing, but started to decline once the treatment was added. In the wells with the drug applied (columns $3-4$ of Fig. 1) the model is able to simultaneously capture the decline of the sensitive population and growth of the resistant population.

In the wells where the sizes of the sensitive and the resistant populations differ significantly, the model fitted the dynamics of the larger population

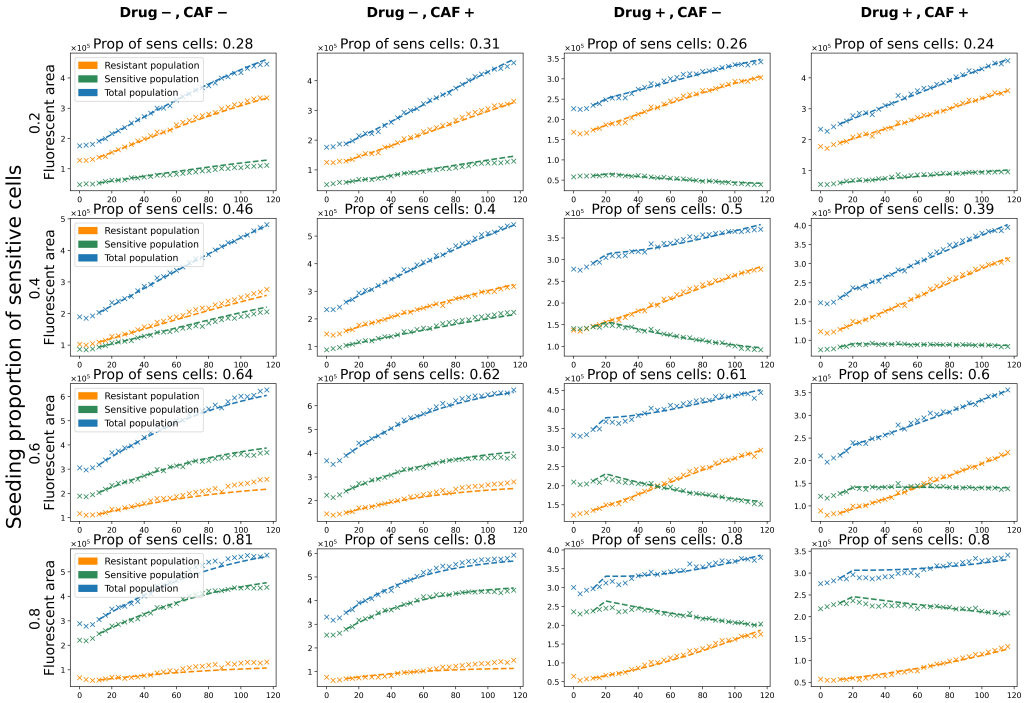

Figure 1: Fit of the polymorphic Gompertzian model to *in vitro* dynamics of sensitive, resistant and total cancer cell populations across four experimental conditions and different initial ratios of sensitive cells. Each graph displays the measured cell counts (crosses) and the model fit (lines) to one well. Sensitive, resistant and total populations are colored in green, orange and blue, respectively. For each well measured proportion of sensitive cells at time point $t = 12h$ (start of the model's fit) is stated above the graph. Columns represent experimental conditions (presence or absence of drug and CAF). Rows contain wells in different conditions with similar initial proportions of sensitive cells.

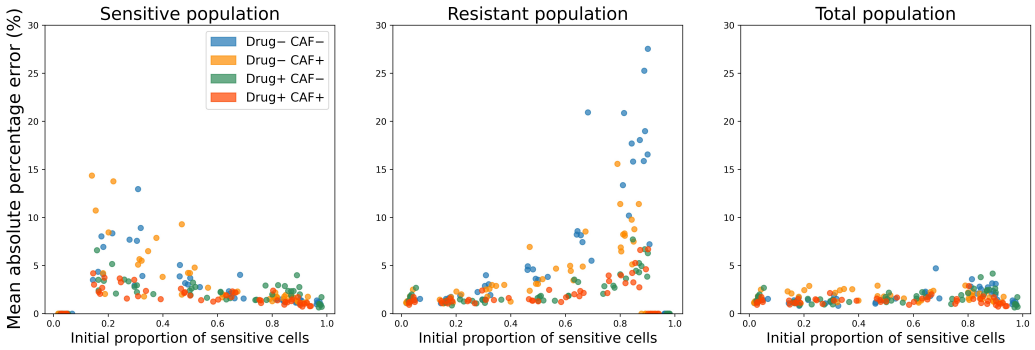

Figure 2: Mean absolute percentage error of the polymorphic Gompertzian model's fit to *in vitro* dynamics of sensitive, resistant and total cancer cell populations across a range of initial proportion of sensitive cells. Data points are colored according to experimental conditions of the well (presence or absence of drug and CAF).

better than the smaller population. This effect is attributed to the common growth rate ρ and carrying capacity K for both sensitive and resistant populations (Eq. (1)- (2)). The optimization problem gave preeminence to the larger population to decrease the total error. While the relative error of the smaller population increased with the decrease of its proportion, the error for the total population stayed below 5% mean absolute percentage error ($MAPE$) for all proportions (Fig. 2). In monotypic wells (seeding proportions of sensitive cells equal 0 or 1) the error of the model's fit to the non-seeded population is 0.

Fig. 2 also shows that in wells with treatment (Drug+, CAF- and Drug+, CAF+), model accuracy was generally higher than in cases without drug. This can be explained by the higher number of parameters in cases with a drug (treatment sensitivity λ was fitted only if treatment was present).

3.1.2. Effect of cancer-associated fibroblasts in the model

Fig. 3 shows model parameters over wells with different initial ratios of sensitive cells and experimental conditions (presence or absence of drug and CAF). The treatment sensitivity parameter λ is significantly smaller in wells where CAF are present, which was confirmed using a Welch's unequal variance t-test (p-value$= 10^{-7}$). Since λ represents the magnitude of drug effect on sensitive cells, smaller values of λ reflect reduced efficiency of the treatment when CAFs are present.

In Fig. 3 we also observe a sudden increase in the fitted carrying capacity

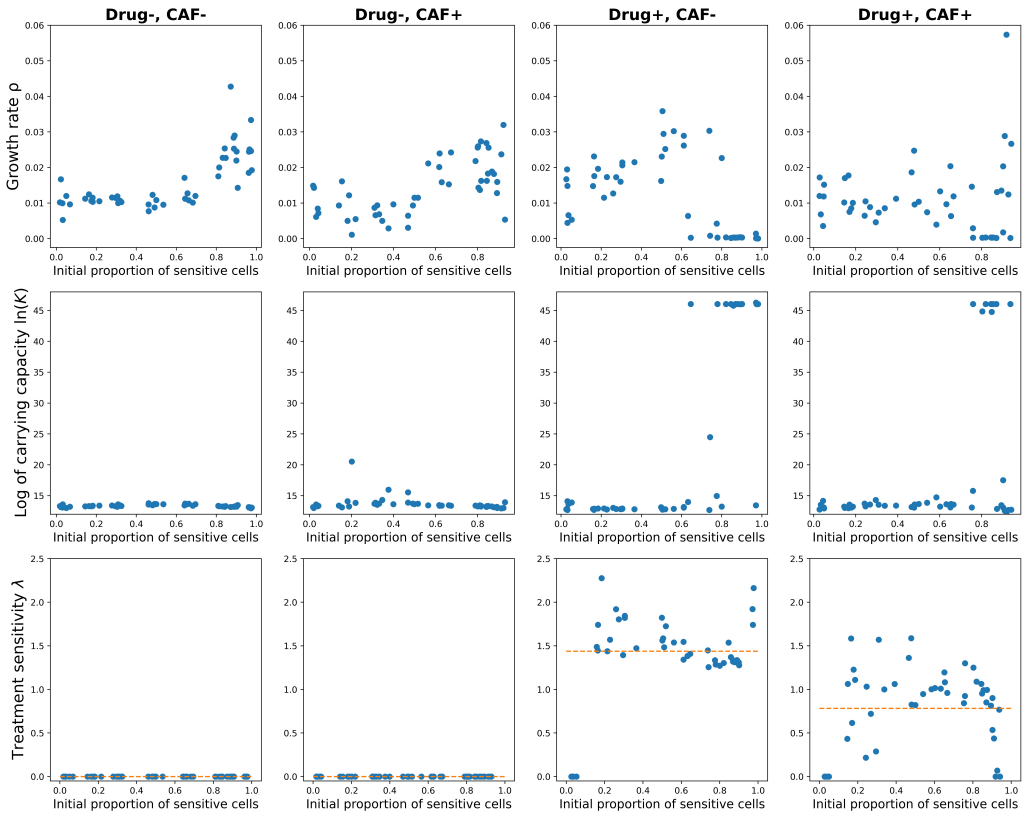

Figure 3: Parameters of the polymorphic Gompertzian model fitted to *in vitro* data across four experimental conditions (indicated in columns) and range of initial proportions of sensitive cells. Each dot in the graphs corresponds to the parameter value of the model fitted to dynamics from one well. The orange line indicates the mean value of treatment sensitivity λ in a given experimental condition.

K and related decay in the fitted growth rate ρ for the majority of wells with $p \geq 0.6$ and drug present. In these cases, a very high K value makes the term $\ln(\frac{K}{N})$ almost constant for the entire measured period (changes in N have nearly no effect, as $K \gg N(t), \forall t$). At the same time, a low growth rate ρ compensates for the magnitude of $\ln(\frac{K}{N})$. Such parameter values result in an exponential growth for resistant population and an exponential decrease for sensitive population, reflecting the trends observed in the data.

3.2. In vivo data

3.2.1. The model's fit to different trend categories

We divided the *in vivo* data into groups based on the displayed trend in tumor growth and evaluated the model's performance in each of these categories (See Section 2.2). Fig. 4 presents the polymorphic Gompertzian model's fit to five representative patient cases from each trend category. The two top rows show that the model can accurately capture both "Growth" and "Decline" trends. In these categories, one of the populations has a significantly larger effect on the total population dynamics. In the "Growth" category, the increase of the tumor size is attributed to the proliferation of the resistant population. In the "Decline" category, in contrast, the sensitive population plays a major role, forming the downward trend of the total population size. The polymorphic Gompertzian model is also successful in describing the "U-shape" trend in the data due to incorporated heterogeneity. In this case, sensitive population initially prevails but then decreases under treatment. As the result, resistant population is able to proliferate without competition for space and resources, which leads to regrowth of the tumor.

In the "Delayed response" category, the model is unable to capture the trend. The model tends to ignore initial tumor size increase and fits the data as a monotonic decline. In some cases, where the response is delayed longer, the model describes it as a growth trend and does not capture the subsequent decline (5th graph in the "Delayed response" row of Fig. 4). In the "Fluctuate" category, the polymorphic Gompertzian model estimates data dynamics with a monotonic growth, a monotonic decline, or a U-shape trend. The model is often able to capture the main tendency in the data but ignores smaller fluctuations.

Overall, the lowest mean errors of the model's fit correspond to "Growth" and "Decline" categories and the highest mean error corresponds to the "Delayed response" trends (See Appendix D). We also conclude that the polymorphic Gompertzian model presents a higher accuracy in the majority of cases

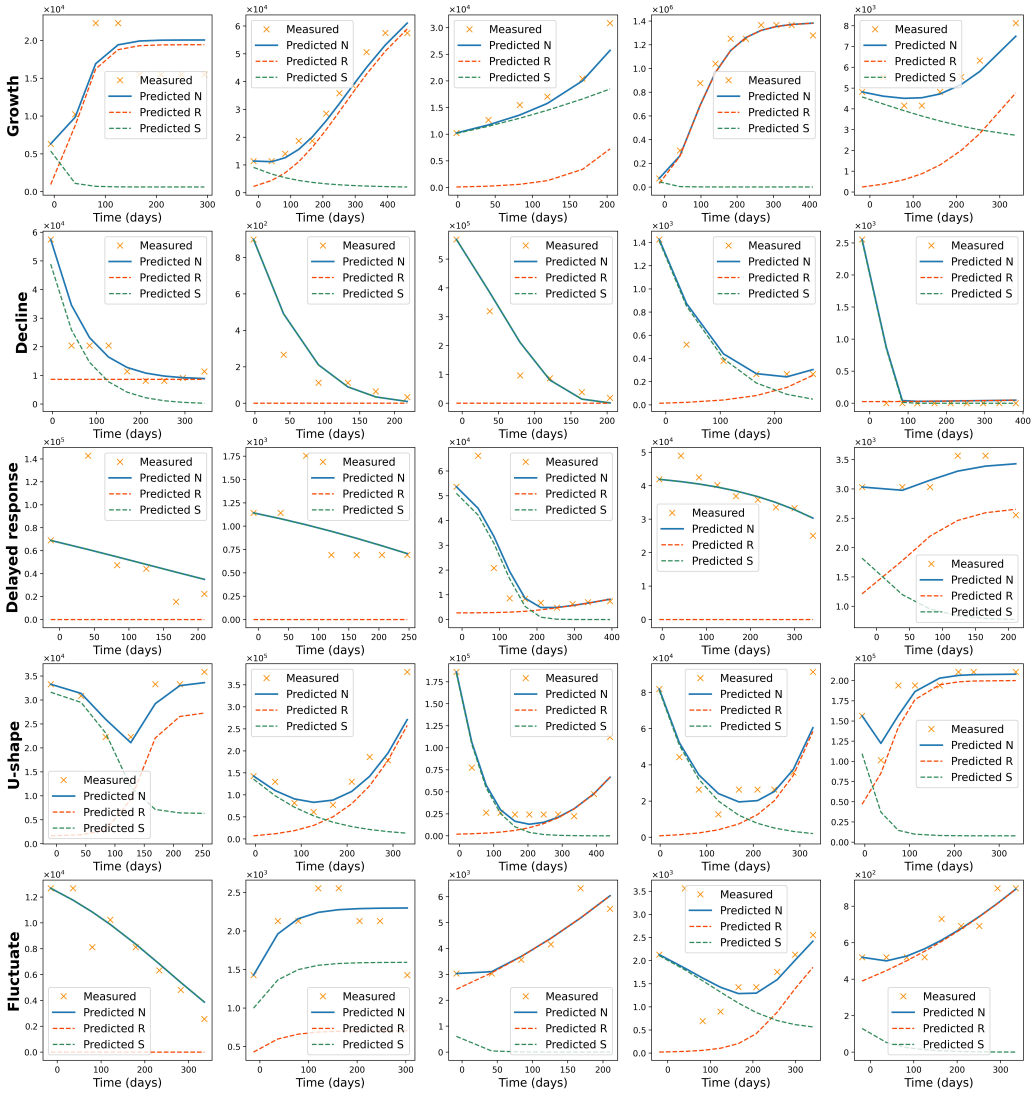

Figure 4: The polymorphic Gompertzian model's fit to *in vivo* data across five trend categories. Each row shows five patient cases corresponding to one of the trend categories: "Growth", "Decline", "Delayed response", "U-shape" or "Fluctuate". Measured tumor volume over time is marked with orange crosses. The blue line represents the model's fit to the total tumor size dynamics, green and orange lines represent predicted dynamics of sensitive and resistant populations sizes respectively.

comparing to the monomorphic Gompertz and General van Bertalanffy models. The mean error of the polymorphic Gompertzian model's fit is smaller than that of the General Gompertz model in the "Growth" and "Decline" categories and similar to that of the General von Bertalanffy model. None of the models is capable of describing the "Delayed response" trend and the error values in this category are similar for all three models. The polymorphic Gompertzian model demonstrates a higher accuracy than the other models in the "U-shape" category (See Appendix C for details).

4. Discussion

We validated the polymorphic Gompertzian model of Viossat and Noble [26] using *in vitro* and *in vivo* data. Overall, the model fits both studied cases very well. The model assumes (i) a shared carrying capacity between sensitive and resistant cell populations, (ii) the growth rate of the two populations being equal in the absence of drug, and (iii) no competition/cooperation effects in terms of a competition/fitness matrix. Due to these assumptions we were not able to confirm all conclusions of Kazatcheev et al's game-theoretic model [30]. The polymorphic Gompertzian model may be however perceived as implicitly frequency-dependent in *in vitro* case, as we fitted the model's parameters separately for different initial proportions of sensitive cells. Nevertheless, the model's assumptions allowed it to fit both the rich data from *in vitro* experiments and the sparse data from *in vivo* clinical studies.

With the polymorphic Gompertzian model, we took a conceptually different approach to the analysis of the Kaznatcheev et al. [30] *in vitro* data. Kaznatcheev et al. [30] specifically designed a new experimental procedure as a way to measure a competition/fitness matrix [42] that allowed for two distinct fitness functions for the sensitive and resistant cell types. We showed that the polymorphic Gompertzian model could describe this well with a growth rate ρ that is the same for the sensitive and resistant types. We confirmed the anti-treatment effect of cancer-associated fibroblasts. However, we did not confirm Kaznatcheev's et al. [30] conclusion on strong violations of the cost of resistance (where resistant cells are fitter than sensitive cells even outside treatment), as the polymorphic Gompertzian model with a common growth rate ρ does not allow to compare fitness of the populations.

The future work shall consider extensions of the polymorphic Gompertzian model to cases where sensitive and resistant cells are allowed to have different growth rates and/or when frequency-dependent selection is included in

the form of competition matrix. Such extensions can be tested on other existing or proposed *in vitro* datasets that provide data on different cell type proportions [43–46] or population sizes [34, 47, 48].

In this study we demonstrated that the polymorphic Gompertzian model can also be parametrized with the more sparse data from *in vivo* tumor size dynamics of patients undergoing therapy. The polymorphic Gompertzian model provides a good fit of the "Growth" and "Decline" categories, with the error comparable to the error of the best performing classical model of cancer growth – General von Bertalanffy. In the "Growth" category, the polymorphic Gompertzian model described the tumor as consisting mostly of resistant cells. While in the "Decline" category, if the tumor size declines monotonically to zero than the model can treat the cancer population as completely sensitive. However, if the last few measurements show a slight increase in the tumor size, the model indicates that the resistant population is still present – allowing for the possibility of relapse and tumor regrowth. The main advantage of the polymorphic Gompertzian model is its ability to capture relapse and regrowth described clinically by the "U-shape" trend – a trend that cannot be captured by any of the six classical models analyzed by Ghaffari Laleh et al. [34].

The polymorphic Gompertzian model (along with the classic models) does not capture the "Delayed Response" trend for *in vivo* data. This could be due to the lack of information on when exactly treatment started: in the clinical studies, the first measurement of the tumor size was usually performed few days before the treatment started. Thus, the initial growth of the tumor in the "Delayed Response" trend might have happened before treatment was first applied. If we had tumor size measurements on the day the therapy started then we could correct for this. We do exactly this correction for Kaznatcheev et al. [30] *in vitro* data to capture a delayed response effect. Alternatively, the *in vivo* "Delayed Response" trend might be attributed to having insufficient concentration of the drug in the tumor at first injection. In this case, data on drug concentration over time would be required for the polymorphic Gompertzian model to describe these cases through a time dependent treatment variable.

In our study, we demonstrate the ability of the polymorphic Gompertzian model to describe real-world data. Going forward, the most promising future development is modelling real-world time dependent treatment, especially adaptive therapy. The "U-shape" trend that the polymorphic Gompertzian model captures in the *in vivo* data presents an undesirable scenario for the

patients. In 54 out of 81 cases in the "U-shape" category, the tumor regrows to the initial size or greater. The theoretical conclusions of Viossat and Noble [26] suggest that for these cases, the implementation of containment therapy could be beneficial and might prolong the time to tumor progression. Contradictory, Kaznatcheev et al. [30] suggest that there would be little benefit to adaptive therapy given the competition/fitness matrices that they estimated *in vitro*. Of course, in the real-world, the behavior of the tumor under containment therapy may differ from the mathematically predictions and, therefore, the effectiveness of such an adaptive therapy should be tested for the cases analyzed in this paper.

5. Acknowledgments

This research was supported by the European Union's Horizon 2020 research and innovation programme under the Marie Skłodowska-Curie grant agreement No. 955708 and the Dutch National Foundation projects VI.Vidi.213.139 and OCENW.KLEIN.277.

References

[1] A. Jemal, E. M. Ward, C. J. Johnson, K. A. Cronin, J. Ma, A. B. Ryerson, A. Mariotto, A. J. Lake, R. Wilson, R. L. Sherman, et al., Annual report to the nation on the status of cancer, 1975–2014, featuring survival, JNCI: Journal of the National Cancer Institute 109 (9) (2017) djx030. doi:10.1093/jnci/djx030.

[2] A. M. Dujon, A. Aktipis, C. Alix-Panabières, S. R. Amend, A. M. Boddy, J. S. Brown, J.-P. Capp, J. DeGregori, P. Ewald, R. Gatenby, M. Gerlinger, M. Giraudeau, R. K. Hamede, E. Hansen, I. Kareva, C. C. Maley, A. Marusyk, N. McGranahan, M. J. Metzger, A. M. Nedelcu, R. Noble, L. Nunney, K. J. Pienta, K. Polyak, P. Pujol, A. F. Read, B. Roche, S. Sebens, E. Solary, K. Staňková, H. Swain Ewald, F. Thomas, B. Ujvari, Identifying key questions in the ecology and evolution of cancer, Evolutionary Applications 14 (4) (2021) 877–892. doi:10.1111/eva.13190.

[3] R. A. Gatenby, A change of strategy in the war on cancer, Nature 459 (7246) (2009) 508–509. doi:10.1038/459508a.

[4] A. Prasanna, M. M. Ahmed, M. Mohiuddin, C. N. Coleman, Exploiting sensitization windows of opportunity in hyper and hypo-fractionated radiation therapy, Journal of thoracic disease 6 (4) (2014) 287. doi:10.3978/j.issn.2072-1439.2014.01.14.

[5] J. Zhang, J. J. Cunningham, J. S. Brown, R. A. Gatenby, Integrating evolutionary dynamics into treatment of metastatic castrate-resistant prostate cancer, Nature Communications 8 (1) (2017) 1816. doi:10.1038/s41467-017-01968-5.

[6] A. Kaznatcheev, R. Vander Velde, J. G. Scott, D. Basanta, Cancer treatment scheduling and dynamic heterogeneity in social dilemmas of tumour acidity and vasculature, British journal of cancer 116 (6) (2017) 785–792. doi:10.1038/bjc.2017.5.

[7] K. Bacevic, R. Noble, A. Soffar, O. Wael Ammar, B. Boszonyik, S. Prieto, C. Vincent, M. E. Hochberg, L. Krasinska, D. Fisher, Spatial competition constrains resistance to targeted cancer therapy, Nature communications 8 (1) (2017) 1995. doi:10.1038/s41467-017-01516-1.

[8] P. I. Warman, A. Kaznatcheev, A. Araujo, C. C. Lynch, D. Basanta, Fractionated follow-up chemotherapy delays the onset of resistance in bone metastatic prostate cancer, Games 9 (2) (2018) 19. doi:10.3390/g9020019.

[9] N. Yoon, R. Vander Velde, A. Marusyk, J. G. Scott, Optimal therapy scheduling based on a pair of collaterally sensitive drugs, Bulletin of mathematical biology 80 (2018) 1776–1809. doi:10.1007/s11538-018-0434-2.

[10] A. Camacho, S. Jerez, Bone metastasis treatment modeling via optimal control, Journal of mathematical biology 78 (2019) 497–526. doi:10.1007/s00285-018-1281-3.

[11] K. Stanková, J. S. Brown, W. S. Dalton, R. A. Gatenby, Optimizing Cancer Treatment Using Game Theory: A Review, JAMA Oncology 5 (1) (2019) 96. doi:10.1001/jamaoncol.2018.3395.

[12] M. Gluzman, J. G. Scott, A. Vladimirsky, Optimizing adaptive cancer therapy: dynamic programming and evolutionary game theory,

Proceedings of the Royal Society B 287 (1925) (2020) 20192454. doi:10.1098/rspb.2019.2454.

[13] N. Yoon, N. Krishnan, J. Scott, Theoretical modeling of collaterally sensitive drug cycles: shaping heterogeneity to allow adaptive therapy, Journal of Mathematical Biology 83 (2021) 1–29. doi:10.1007/s00285-021-01671-6.

[14] B. Wölfl, H. te Rietmole, M. Salvioli, A. Kaznatcheev, F. Thuijsman, J. S. Brown, B. Burgering, K. Staňková, The contribution of evolutionary game theory to understanding and treating cancer, Dynamic Games and Applications (2021) 1–30doi:10.1007/s13235-021-00397-w.

[15] J. Zhang, J. Cunningham, J. Brown, R. Gatenby, Evolution-based mathematical models significantly prolong response to abiraterone in metastatic castrate-resistant prostate cancer and identify strategies to further improve outcomes, eLife 11 (2022) e76284. doi:10.7554/eLife.76284.

[16] R. A. Gatenby, A. S. Silva, R. J. Gillies, B. R. Frieden, Adaptive Therapy, Cancer Research 69 (11) (2009) 4894–4903. doi:10.1158/0008-5472.CAN-08-3658.

[17] J. J. Cunningham, J. S. Brown, R. A. Gatenby, K. Staňková, Optimal control to develop therapeutic strategies for metastatic castrate resistant prostate cancer, Journal of Theoretical Biology 459 (2018) 67–78. doi:10.1016/j.jtbi.2018.09.022.

[18] A. S. Silva, Y. Kam, Z. P. Khin, S. E. Minton, R. J. Gillies, R. A. Gatenby, Evolutionary Approaches to Prolong Progression-Free Survival in Breast Cancer, Cancer Research 72 (24) (2012) 6362–6370. doi:10.1158/0008-5472.CAN-12-2235.

[19] R. Martin, M. Fisher, R. Minchin, K. Teo, Optimal control of tumor size used to maximize survival time when cells are resistant to chemotherapy, Mathematical Biosciences 110 (2) (1992) 201–219. doi:10.1016/0025-5564(92)90038-X.

[20] H. C. Monro, E. A. Gaffney, Modelling chemotherapy resistance in palliation and failed cure, Journal of Theoretical Biology 257 (2) (2009) 292–302. doi:10.1016/j.jtbi.2008.12.006.

[21] M. Pressley, M. Salvioli, D. B. Lewis, C. L. Richards, J. S. Brown, K. Staňková, Evolutionary dynamics of treatment-induced resistance in cancer informs understanding of rapid evolution in natural systems, Frontiers in Ecology and Evolution 9 (2021) 460. doi:10.3389/fevo.2021.681121.

[22] P. Bayer, R. A. Gatenby, P. H. McDonald, D. R. Duckett, K. Staňková, J. S. Brown, Coordination games in cancer, PLOS ONE 17 (1) (2022) 1–15. doi:10.1371/journal.pone.0261578.

[23] A. Stein, M. Salvioli, H. Garjani, J. Dubbeldam, Y. Viossat, J. S. B. K. Staňková, Stackelberg evolutionary game theory: How to manage evolving systems, Philosophical Transactions of the Royal Society B 378 (1876) (2023). doi:10.1098/rstb.2021.0495.

[24] J. Zhang, J. J. Cunningham, J. S. Brown, R. A. Gatenby, Evolution-based mathematical models significantly prolong response to abiraterone in metastatic castrate-resistant prostate cancer and identify strategies to further improve outcomes, Elife 11 (2022) e76284. doi:10.7554/eLife.76284.

[25] P. Bayer, J. West, Games and the treatment convexity of cancer, bioRxiv (2023). doi:10.1101/2023.02.27.530257.

[26] Y. Viossat, R. Noble, A theoretical analysis of tumour containment, Nature Ecology & Evolution 5 (6) (2021) 826–835. doi:10.1038/s41559-021-01428-w.

[27] K. Staňková, Resistance games, Nature Ecology & Evolution 3 (3) (2019) 336–337. doi:10.1038/s41559-018-0785-y.

[28] Y. Kam, T. Das, H. Tian, P. Foroutan, E. Ruiz, G. Martinez, S. Minton, R. J. Gillies, R. A. Gatenby, Sweat but no gain: Inhibiting proliferation of multidrug resistant cancer cells with "ersatzdroges": Inhibiting MDR cancer cells with ersatzdroges, International Journal of Cancer 136 (4) (2015) E188–E196. doi:10.1002/ijc.29158.

[29] M. Pressley, M. Salvioli, D. B. Lewis, C. L. Richards, J. S. Brown, K. Staňková, Evolutionary Dynamics of Treatment-Induced Resistance in Cancer Informs Understanding of Rapid Evolution in Nat-

ural Systems, Frontiers in Ecology and Evolution 9 (2021) 681121. doi:10.3389/fevo.2021.681121.

[30] A. Kaznatcheev, J. Peacock, D. Basanta, A. Marusyk, J. G. Scott, Fibroblasts and alectinib switch the evolutionary games played by non-small cell lung cancer, Nature Ecology & Evolution 3 (3) (2019) 450–456. doi:10.1038/s41559-018-0768-z.

[31] M. A. Strobl, J. West, Y. Viossat, M. Damaghi, M. Robertson-Tessi, J. S. Brown, R. A. Gatenby, P. K. Maini, A. R. Anderson, Turnover modulates the need for a cost of resistance in adaptive therapy, Therapy. Cancer Res. 81 (4) (2021) 1135–1147. doi:10.1158/0008-5472.CAN-20-0806.

[32] R. Brady, H. Enderling, Mathematical Models of Cancer: When to Predict Novel Therapies, and When Not to, Bulletin of Mathematical Biology 81 (10) (2019) 3722–3731. doi:10.1007/s11538-019-00640-x.

[33] N. D. Lee, K. Kaveh, I. Bozic, Clonal interactions in cancer: integrating quantitative models with experimental and clinical data, in: Seminars in Cancer Biology, Vol. 92, Elsevier, 2023, pp. 61–73. doi:10.1016/j.semcancer.2023.04.002.

[34] N. Ghaffari Laleh, C. M. L. Loeffler, J. Grajek, K. Staňková, A. T. Pearson, H. S. Muti, C. Trautwein, H. Enderling, J. Poleszczuk, J. N. Kather, Classical mathematical models for prediction of response to chemotherapy and immunotherapy, PLOS Computational Biology 18 (2) (2022) e1009822. doi:10.1371/journal.pcbi.1009822.

[35] D. R. Spigel, J. E. Chaft, S. Gettinger, B. H. Chao, L. Dirix, P. Schmid, L. Q. Chow, R. J. Hicks, L. Leon, J. Fredrickson, M. Kowanetz, A. Sandler, R. Funke, N. A. Rizvi, FIR: Efficacy, Safety, and Biomarker Analysis of a Phase II Open-Label Study of Atezolizumab in PD-L1–Selected Patients With NSCLC, Journal of Thoracic Oncology 13 (11) (2018) 1733–1742. doi:10.1016/j.jtho.2018.05.004.

[36] L. Fehrenbacher, A. Spira, M. Ballinger, M. Kowanetz, J. Vansteenkiste, J. Mazieres, K. Park, D. Smith, A. Artal-Cortes, C. Lewanski, F. Braiteh, D. Waterkamp, P. He, W. Zou, D. S. Chen, J. Yi, A. Sandler, A. Rittmeyer, Atezolizumab versus docetaxel for patients with previously treated non-small-cell lung cancer (POPLAR): a multicentre,

open-label, phase 2 randomised controlled trial, The Lancet 387 (10030) (2016) 1837–1846. doi:10.1016/S0140-6736(16)00587-0.

[37] S. Peters, S. Gettinger, M. L. Johnson, P. A. Jänne, M. C. Garassino, D. Christoph, C. K. Toh, N. A. Rizvi, J. E. Chaft, E. Carcereny Costa, J. D. Patel, L. Q. Chow, M. Koczywas, C. Ho, M. Früh, M. van den Heuvel, J. Rothenstein, M. Reck, L. Paz-Ares, F. A. Shepherd, T. Kurata, Z. Li, J. Qiu, M. Kowanetz, S. Mocci, G. Shankar, A. Sandler, E. Felip, Phase II Trial of Atezolizumab As First-Line or Subsequent Therapy for Patients With Programmed Death-Ligand 1–Selected Advanced Non–Small-Cell Lung Cancer (BIRCH), Journal of Clinical Oncology 35 (24) (2017) 2781–2789. doi:10.1200/JCO.2016.71.9476.

[38] A. Rittmeyer, F. Barlesi, D. Waterkamp, K. Park, F. Ciardiello, J. von Pawel, S. M. Gadgeel, T. Hida, D. M. Kowalski, M. C. Dols, D. L. Cortinovis, J. Leach, J. Polikoff, C. Barrios, F. Kabbinavar, O. A. Frontera, F. De Marinis, H. Turna, J.-S. Lee, M. Ballinger, M. Kowanetz, P. He, D. S. Chen, A. Sandler, D. R. Gandara, Atezolizumab versus docetaxel in patients with previously treated non-small-cell lung cancer (OAK): a phase 3, open-label, multicentre randomised controlled trial, The Lancet 389 (10066) (2017) 255–265. doi:10.1016/S0140-6736(16)32517-X.

[39] L. Beal, D. Hill, R. Martin, J. Hedengren, GEKKO Optimization Suite, Processes 6 (8) (2018) 106. doi:10.3390/pr6080106.

[40] E. Sahai, I. Astsaturov, E. Cukierman, D. G. DeNardo, M. Egeblad, R. M. Evans, D. Fearon, F. R. Greten, S. R. Hingorani, T. Hunter, R. O. Hynes, R. K. Jain, T. Janowitz, C. Jorgensen, A. C. Kimmelman, M. G. Kolonin, R. G. Maki, R. S. Powers, E. Puré, D. C. Ramirez, R. Scherz-Shouval, M. H. Sherman, S. Stewart, T. D. Tlsty, D. A. Tuveson, F. M. Watt, V. Weaver, A. T. Weeraratna, Z. Werb, A framework for advancing our understanding of cancer-associated fibroblasts, Nature Reviews Cancer 20 (3) (2020) 174–186. doi:10.1038/s41568-019-0238-1.

[41] A. Faustino-Rocha, P. A. Oliveira, J. Pinho-Oliveira, C. Teixeira-Guedes, R. Soares-Maia, R. G. da Costa, B. Colaço, M. J. Pires, J. Colaço, R. Ferreira, M. Ginja, Estimation of rat mammary tumor volume using caliper and ultrasonography measurements, Lab Animal 42 (6) (2013) 217–224. doi:10.1038/laban.254.

[42] A. Kaznatcheev, C.-H. Lin, Measuring as a new mode of inquiry that bridges evolutionary game theory and cancer biology, Philosophy of Science 89 (5) (2022) 1124–1133. doi:10.1017/psa.2022.57.

[43] M. Archetti, D. A. Ferraro, G. Christofori, Heterogeneity for igf-ii production maintained by public goods dynamics in neuroendocrine pancreatic cancer, Proceedings of the National Academy of Sciences 112 (6) (2015) 1833–1838. doi:10.1073/pnas.1414653112.

[44] R. Bhattacharya, R. Vander Velde, V. Marusyk, B. Desai, A. Kaznatcheev, A. Marusyk, D. Basanta, Understanding the evolutionary games in nsclc microenvironment, bioRxiv (2020) 2020–11doi:10.1101/2020.11.30.404350.

[45] R. J. Noble, V. Walther, C. Roumestand, M. E. Hochberg, U. Hibner, P. Lassus, Paracrine behaviors arbitrate parasite-like interactions between tumor subclones, Frontiers in ecology and evolution 9 (2021) 675638. doi:10.3389/fevo.2021.675638.

[46] N. Farrokhian, J. Maltas, M. Dinh, A. Durmaz, P. Ellsworth, M. Hitomi, E. McClure, A. Marusyk, A. Kaznatcheev, J. G. Scott, Measuring competitive exclusion in non–small cell lung cancer, Science Advances 8 (26) (2022) eabm7212. doi:10.1126/sciadv.abm7212.

[47] H. Cho, A. L. Lewis, K. M. Storey, H. M. Byrne, Designing experimental conditions to use the lotka–volterra model to infer tumor cell line interaction types, Journal of Theoretical Biology 559 (2023) 111377. doi:10.1016/j.jtbi.2022.111377.

[48] M. Strobl, A. Martin, J. West, J. Gallaher, M. Robertson-Tessi, R. Gatenby, R. Wenham, P. Maini, M. Damaghi, A. R. Anderson, Adaptive therapy for ovarian cancer: An integrated approach to parp inhibitor scheduling, bioRxiv (2023) 2023–03doi:10.1101/2023.03.22.533721.